

# Efficient Control Management of Dynamic Voltage Restorer using Feedback Controller

Sushil Kumar <sup>1</sup>, Varsha Mehar <sup>2</sup><sup>1,2</sup>Department of Electrical Engineering, RKDF University, Bhopal, India

\* Corresponding Author: Sushil Kumar

Manuscript Received:

Manuscript Accepted:

**Abstract:** In this paper, novel efficient control management of dynamic voltage restorer using feedback controller is presented as a primary power quality problem and a series connected converter is considered to be an effective and cost-effective solution to mitigate voltage dips. The main aim of this paper is the efficient design and control of a dynamic voltage restorer (DVR) using feedback controller. The DVR is a series connected device, which primarily can protect sensitive electric consumers against voltage dips and surges in the medium and low voltage distribution grid.

**Keywords:** Dynamic Voltage Restorer, Controlling Devices, Voltage Harmonics, Voltage Dip

## I Introduction

The dynamic voltage restorer is a series connected device, which by voltage injection can control the load voltage. In the case of a voltage dip the DVR injects the missing voltage and it avoids any tripping the load. Figure 1 illustrates the operation principle of a DVR. The dynamic voltage restorer (DVR) discovers and compensates for sags in the voltage

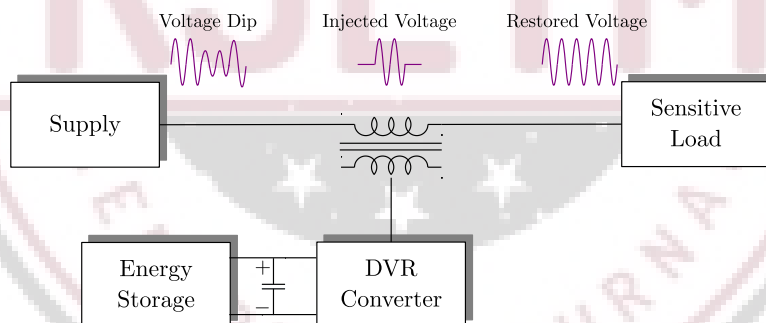


Figure 1: Dynamic Voltage Restorer for Load Voltage and Sensitive Load

of the AC power source so that the loads are insulated from these power reliability issues. The operating principle for the DVR is illustrated in Figure 2. The DVR consists of DC power sources, an insulated-gate bipolar transistor (IGBT) converter, and an injection transformer which is connected in series with the power line and the sensitive load. The DC power sources that can be used are batteries, super-capacitors, superconducting magnetic storage units, and flywheels. A sag in the input AC power line voltage may propagate through the power network due to a fault in one of the distribution feeder lines. The DVR detects the sag and generates AC power from the DC power source by using the insulated-gate bipolar transistor (IGBT) converter. The generated power is fed to the line by the transformer to correct the sag so that the sensitive load receives a highly reliable AC input power.

### I-A Basic Components of a Dynamic Voltage Restorer (DVR)

Figure 3 illustrates some of the basic elements of a DVR, which are:

- **Converter:** The converter is most likely a voltage source converter (VSC), which pulse width modulates (PWM) the DC from the DC-link/storage to AC-voltages injected into the system.

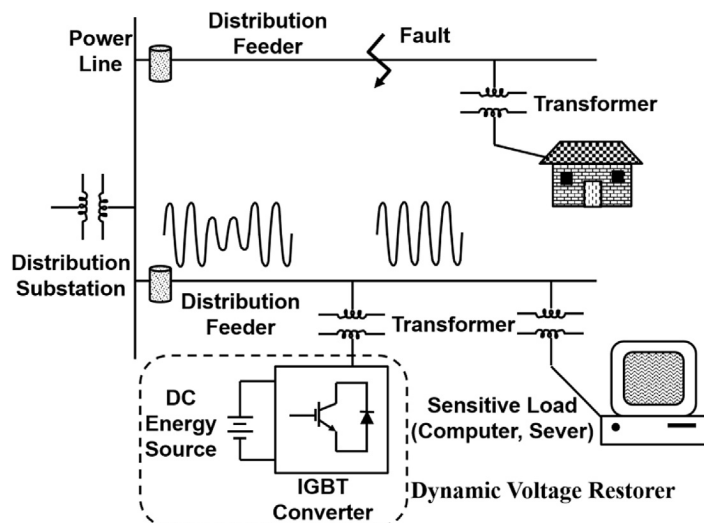


Figure 2: Operating Principle of Dynamic Voltage Restorer

- **Line-Filter:** The line-filter is inserted to reduce the switching harmonics generated by the PWM VSC.
- **Injection Transformer:** In most DVR applications the DVR is equipped with injection transformers to ensure galvanic isolation and to simplify the converter topology and protection equipment.
- **DC-link and Energy Storage:** A DC-link voltage is used by the voltage source converter (VSC) to synthesize an AC voltage into the grid and during a majority of voltage dips active power injection is necessary to restore the supply voltages.
- **By-Pass Equipment:** During faults, overload and service a bypass path for the load current has to be ensured. Illustrated in Figure 3 as a mechanical bypass and a thyristor bypass.
- **Disconnection Equipment:** To completely disconnect the DVR during service etc.

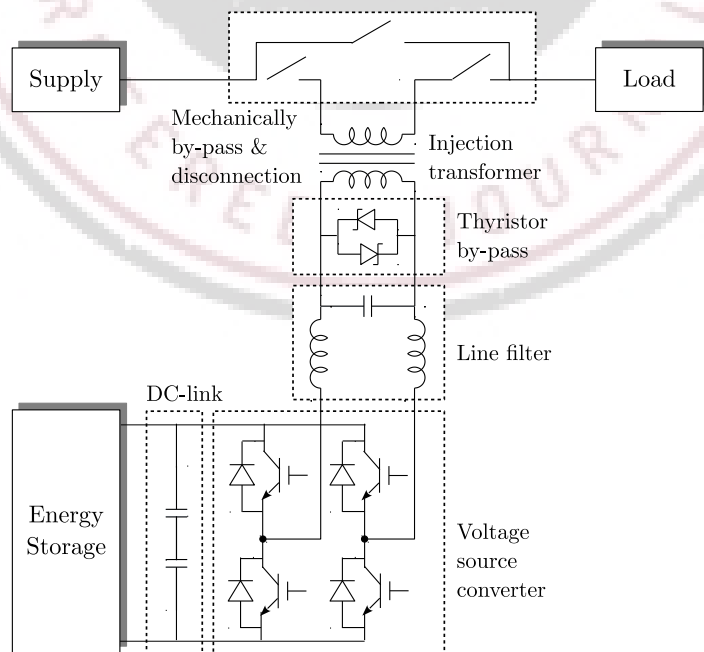


Figure 3: The Basic Elements of a DVR in a Single-Phase Representation

## II Related Work

### II-A Real-Time Implementation of Transformerless Dynamic Voltage Restorer based on T-Type Multilevel Inverter with Reduced Switch Count

Rajkumar *et al.* [1] explained the design and development of a T-type multilevel inverter (MLI) topology for the application of transformerless DVR to alleviate the voltage swell and voltage sag are . The advantage of this topology is to reduce the number of switches compared with other conventional topologies. Transformerless DVR leads to reduced cost and difficulty of the DVR. The performance and the efficiency of the proposed DVR are verified by simulation results as well as real-time prototype setup with OPAL-RT results. In addition, the DVR is controlled by abc to dq controller. The capability of the five-level T-type MLI-based DVR is tested using in-phase compensation technique with reduced carrier PWM scheme to improve THD in line voltages. The proposed DVR is able to keep the load current and voltage THD under the specified limits of IEEE-1159 standard. Also, the compensation capability of the proposed DVR is very fast in compensating the voltage sag and voltage swell.

#### II-A.1 DVR Controller using abc to dq Rotating Frame

Two controllers are well-known in a linear control system, open loop (feedforward), and closed loop (feedback). Feedforward controller is faster than feedback controller for the required voltage compensation. The feedback controllers are best in minimizing the steady-state error.

Block diagram of abc to dq control technique is shown in Figure 4 in which the measured three-phase grid voltages are transformed from abc to dq rotating frame using abc/dq transform with support of PLL. The reference value of DVR in dq frame is obtained by subtracting grid voltage  $V_{g,d}$  and  $V_{g,q}$  from their respective reference values. These reference values generated based on in-phase compensation technique. The obtained DVR reference voltages transformed back to abc components using dq/abc transformation. The reference voltages can be considered as reference signals for PWM modulation.

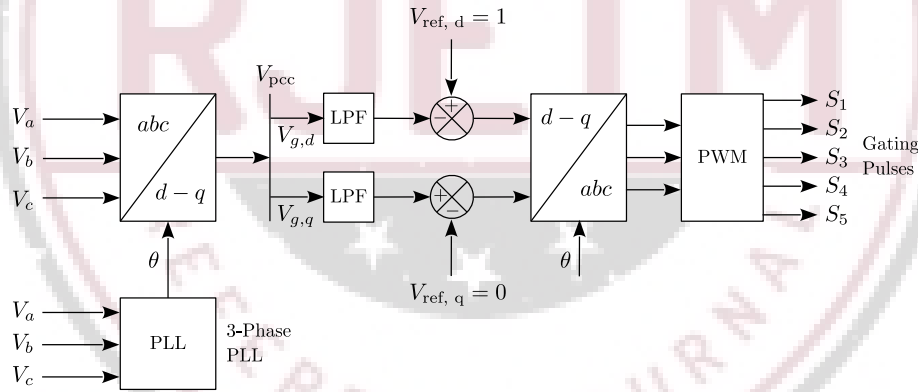


Figure 4: abc to dq Control Technique for 3-Phase Dynamic Voltage Restorer (DVR)

#### II-A.2 Mathematical Analysis of abc – dq Rotating Frame

In  $d - q$  transformation, the  $3 - \phi$  system is transformed to the  $2 - \phi$  stationary reference frame, and then these variables stationary frame to a rotary reference frame with an angular velocity of “ $\omega$ ”. Deduce the  $dq0$  components from abc signals by performing an abc to dq0 transformation in a rotating reference frame by using Equation 1.

$$\begin{bmatrix} V_d \\ V_q \\ V_0 \end{bmatrix} = \frac{2}{3} \begin{bmatrix} \cos \theta & \cos \left( \theta - \frac{2\pi}{3} \right) & \cos \left( \theta + \frac{2\pi}{3} \right) \\ \sin \theta & -\sin \left( \theta - \frac{2\pi}{3} \right) & -\sin \left( \theta + \frac{2\pi}{3} \right) \\ \frac{1}{2} & \frac{1}{2} & \frac{1}{2} \end{bmatrix} \begin{bmatrix} V_a \\ V_b \\ V_c \end{bmatrix} \quad (1)$$

The reference voltages of the DVR in the  $dq0$  frame can be expressed in Equation 2 and 3.

$$V_{Dd}^* = V_d^* - V_d \quad (2)$$

$$V_{Dq}^* = V_q^* - V_q \quad (3)$$

DVR reference voltages are obtained by using inverse parks transformation from Equation 4.

$$\begin{bmatrix} V_{dvr\ a}^* \\ V_{dvr\ b}^* \\ V_{dvr\ c}^* \end{bmatrix} = \begin{bmatrix} \cos \theta & -\sin \theta & 1 \\ \cos(\theta - \frac{2\pi}{3}) & -\sin(\theta - \frac{2\pi}{3}) & 1 \\ \cos(\theta + \frac{2\pi}{3}) & -\sin(\theta + \frac{2\pi}{3}) & 1 \end{bmatrix} \begin{bmatrix} V_{Dd}^* \\ V_{Dq}^* \\ V_{D0}^* \end{bmatrix} \quad (4)$$

## II-B Virtual Impedance Control for a Regional Dynamic Voltage Restorer

Jian *et al.* [2] proposed a novel virtual impedance control strategy that can allow a regional compensation DVR to behave as a virtual series RL or RC element. With properly tuned parameters, a DVR can be operated as a virtual inductor to function as an FCL to limit the fault current of a downstream fault, and can be operated as a virtual capacitor to function as an SC to compensate the voltage loss along a feeder line. A stability analysis shows that a DVR system operating under virtual impedance control is stable for the arbitrary values and types of the load impedance and virtual impedance of the DVR. Simulations and experimental results obtained using a prototype DVR verify the feasibility and effectiveness of the proposed method. Going forward, experiments on a 5MW industrial DVR device will be conducted to further demonstrate the effectiveness of this method.

### II-B.1 Virtual Impedance Control Strategy

Feed-forward control, feedback control, and composite control are the commonly used linear control methods for DVRs [3, 4]. To address the resonance problem associated with the single-stage output LC filter and to improve the stability and adaptability of the DVR, a dual-loop control scheme consisting of an outer capacitor voltage feed-forward loop and an inner inductor current feedback loop is adopted in this research. The corresponding control block diagram is shown in Figure 5.

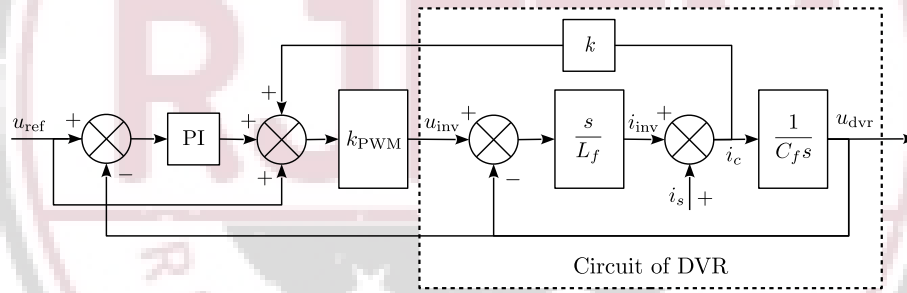


Figure 5: the Dual-Loop Control

In Figure 5,  $u_{ref}$  is the reference voltage of the DVR, the PI controller is expressed as  $k_p + k_i/s$ ;  $k_{PWM}$  is the attenuation coefficient of the DVR inverter;  $L_f$  and  $C_f$  are the inductance and capacitance, respectively, of the LC filter; and  $k$  is the current feedback coefficient.

The transfer function of the dual-loop control system shown can be derived as follows:

$$u_{dvr} = \frac{(k_{PWM}(k_p + 1)s + k_{PWM}k_i)u_{ref} - L_f s^2 i_s}{L_f C_f s^3 + k_{PWM} k C_f s^2 + (k_{PWM} k_p + 1)s + k_{PWM} k_i} \quad (5)$$

A downstream fault of the DVR may cause the bus voltage  $u_s$  to decrease and a large fault current to flow through the feeder line. If the DVR responds to this voltage sag, a current larger than that before compensation will flow through the DVR, which may threaten the safety of the DVR. Therefore, a DVR typically ignores the voltage sags caused by downstream faults and remains in the by-pass mode. However, if we control the DVR such that it is operating with the characteristic of an inductor, then it can serve as an FCL during downstream faults. In this way, not only can the fault current be limited but the subsequent voltage sag on the loads of the other feeders of the same bus can also be avoided.

Controlling the DVR to behave as a resistor  $R_0$  in series with an inductor  $L_0$  means

$$u_{ref} = (R_0 + sL_0) i_s \quad (6)$$

Eliminating the variable  $u_{ref}$  by substituting Equation 6 into Equation 5 leads to

$$\frac{u_{dvr}}{i_s} = \frac{g_2 s^2 + g_1 s + g_0}{a_3 s^3 + a_2 s^2 + a_1 s + a_0} \quad (7)$$

where,

$$\begin{aligned}
 g_2 &= k_{\text{PWM}}(k_p + 1)L_0 - L_f, \\
 g_1 &= k_{\text{PWM}}(k_i L_0 + (k_p 1)R_0)L_0, \\
 g_0 &= k_{\text{PWM}}k_i R_0, \\
 a_3 &= L_f C_f, \\
 a_2 &= k_{\text{PWM}}k C_f, \\
 a_1 &= k_{\text{PWM}}k_p + 1, \\
 a_0 &= k_{\text{PWM}}k_i
 \end{aligned}$$

The value of the virtual inductance that the DVR to be controlled as is dependent on the fault features especially the downstream fault impedance.

## II-C Topologies and Control Strategies Implicated in Dynamic Voltage Restorer (DVR) for Power Quality Improvement

Pal and Gupta [5] presented a detailed study on DVR with the different possible configurations of its power circuit and control techniques encircling major power quality issues. The informative object covered in the paper, articulate choice of control strategy and power circuit ensuring optimal recital of DVR in satisfying a required quality. This paper also furnishes the valued information for the investigator in this field.

### II-C.1 In-phase Injection/Compensation Technique

In this technique, DVR injects voltage in-phase with the supply voltage. This technique is suggested for the linear load where voltage magnitude is only essential for compensation. Therefore, the amount of the injected voltage is least due to which the voltage rating of the DC storage system/DC link is minimal.

$$\begin{aligned}
 V_{\text{DVR}} &= V_{\text{inj}} \\
 |V_{\text{inj}}| &= |V_{\text{pre-sag}}| - |V_{\text{sag}}|
 \end{aligned} \tag{8}$$

$$\angle V_{\text{inj}} = \theta_{\text{inj}} = \theta_s \tag{9}$$

This needs real power during compensation but cannot restore the phase angle jump [6–9].

### II-C.2 Pre-Sag Injection/Compensation Technique

In this technique, DVR maintains load voltage phasor unchanged in relation to that before the disturbance. This technique is suggested for the nonlinear load, i.e., sensitive to phase angle jump. It restores both the voltage sag and the phase angle jump. It also avoids any circulating or transient current at the load side.

$$\begin{aligned}
 V_{\text{pre-sag}} &= V_L, V_{\text{sag}} = V_s, V_{\text{DVR}} \\
 |V_{\text{inj}}| &= |V_{\text{pre-sag}}| - |V_{\text{sag}}|
 \end{aligned} \tag{10}$$

$$\theta_{\text{inj}} = \tan^{-1} \left\{ \frac{V_{\text{pre-sag}} \sin(\theta_{\text{pre-sag}})}{V_{\text{pre-sag}} \cos(\theta_{\text{pre-sag}}) - V_{\text{sag}} \cos(\theta_{\text{sag}})} \right\} \tag{11}$$

It needs real power during compensation.

## II-D Dynamic Voltage Restorer With an Improved Strategy to Voltage Sag Compensation and Energy Self-Recovery

Tu *et al.* [10] presented an adaptive scheme for DVR to voltage sag compensation and energy self-recovery. The adaptive schemes improve the voltage quality of sensitive loads by protecting them during grid voltage sags with phase angle jump. The optimized energy self-recovery strategy recovers the DC link voltage and mitigate the phase jump in energy

self-recovery stage as well. Further, the updated procedure for injected reference voltage ensures the DVR system is adapted to different working cases. The simulation and the experimental results of DVR under different cases verify the effectiveness of the proposed strategy.

### II-D.1 Energy Self-Recovery Operation Principle

In energy recovery stage, the most key issue is manage the DC link voltage to reference value and realize the smooth access of DVR to the maximum power operating point. The energy storage using super-capacitor on DC link side, and the voltage of the super-capacitor is determined to be the standard for energy self-recovery stage starting up, a smooth transition is needed to achieve the maximum energy absorption of DVR. The  $\theta_{init}$  and  $\theta_{stable}$  are the initial and steady state phase angle of  $U_{inj}$ , respectively, the slope of the transition curve is determined by  $\Delta t_3$ . Then we can get  $\theta_{init} = 0$  and  $\theta_{stable} = \gamma$ , the transition is defined from initial operating points to the final one, as given in the following:

$$\theta_{dvr} = \theta_{init} + \left( \frac{\theta_{stable} - \theta_{init}}{\Delta t_3} \right) t \quad (12)$$

$$= \frac{\gamma}{\Delta t_3} t \quad (13)$$

Once the energy self-recovery stage is completed, the transition is initiated.

## II-E Power Conditioning using Dynamic Voltage Restorers under Different Voltage Sag Types

Saeed *et al.* [11] presented modeling of DVR for voltage correction using MATLAB software. The performance of the device under different voltage sag types is described. Various power quality indices are used to evaluate the performance of the grid with the proposed device. Several simulation results are introduced to validate that the proposed DVR operation scheme fulfills the required goals. It is obvious that the DVR is capable of effective correction of the voltage sag while minimizing the grid voltage unbalance and harmonics distortion, regardless of the fault type.

### II-E.1 Voltage Sag Lost Energy Index

During voltage sag, the voltage is below normal for some period of time, which reduces the energy delivered to the loads. This index gives the lost energy  $W$  during a sag event, which is defined as follows:

$$W = \sum_{p=a,b,c} W_p \quad (14)$$

$$= \sum_{p=a,b,c} T_p \cdot \left( 1 - \frac{V_p}{V_{nominal}} \right)^\pi \quad (15)$$

where  $V_p$  is a phase voltage per unit with respect to the nominal voltage  $V_{nominal}$  during the sag event, and  $T_p$  is the sag duration in milliseconds for each phase.

## II-F Novel Sag Detection Method for Line-Interactive Dynamic Voltage Restorer

Bae *et al.* [12] proposed a novel sag detection method for the line-interactive dynamic voltage restorer, using instantaneous and rms variation. The proposed method can detect and compensate the voltage interruption within 2 ms delay, which is faster than the existing 4 ms delay. The feasibility of proposed method was verified through computer simulations. The DVR with proposed detection method can effectively compensate the voltage sag or interruption for sensitive loads.

### II-F.1 Line-Interactive Dynamic Voltage Restorer

The measured input voltage is converted into a unit sine signal passing through the phase-locked loop. The reference value of instantaneous sag detection is determined by 0.9 p.u. around the peak point, and zero around the zero-crossing point. The reference value  $v_{sag-ref}$  can be represented by:

$$v_{sag-ref} = \begin{cases} 0.9 \times \sin \omega t & [\theta_1 \leq \omega t \leq \pi - \theta_1] \\ 0 & [-\theta_1 < \omega t < \theta_1] \end{cases} \quad (16)$$

where  $\theta_1$  is  $24.5^\circ$ , and the sine value at  $\theta_1$  is 0.3. The arbitrary source voltage  $v(t)$  can be generally expressed by Equation 17 using the Fourier series.

$$v(t) = \frac{a_0}{2} + \sum_{n=0}^{\infty} a_n \cos n\omega_0 t + \sum_{n=0}^{\infty} b_n \sin n\omega_0 t \quad (17)$$

Applying discrete Fourier transform (DFT) for the fundamental component, Equation 18 and 18 are obtained by separating the real part and imaginary part.

$$a_1 = \frac{\sqrt{2}}{N} \sum_{i=0}^N v \left( t - i \frac{T}{N} \right) \cos \left( 2\pi \frac{i}{N} \right) \quad (18)$$

$$b_1 = \frac{\sqrt{2}}{N} \sum_{i=0}^N v \left( t - i \frac{T}{N} \right) \sin \left( 2\pi \frac{i}{N} \right) \quad (19)$$

Using the value of  $a_1$  and  $b_1$  the rms value of fundamental component can be easily calculated by Equation 20 as

$$v^{1st} = \sqrt{a_1^2 + b_1^2} \quad (20)$$

A hybrid detection method which is composed of the instantaneous detection and the rms variation detection with sliding mode.

## II-G A Two Degrees of Freedom Resonant Control Scheme for Voltage-Sag Compensation in Dynamic Voltage Restorers

Torres *et al.* [13] presents a control scheme based on two nested controllers for voltage sag compensation in a DVR. The nested regulators provide the control with two degrees of freedom, and the control scheme is implemented in the stationary reference frame. Furthermore, in order to accomplish the requirements for voltage sag compensation, it is necessary to track the component at the fundamental frequency. This is achieved using a resonant term in one of the controllers.

The proposed control design methodology is able to define all the poles of the closed-loop system without observers and with a reduction in the number of variables that must be measured, thus making it possible to avoid the use of the traditional current loop employed in control schemes for the DVR. The structure with the nested regulators achieves perfect zero tracking error at the nominal frequency and blocks the DC offset, signifying that it has some advantages over other control methods, such as double-loop schemes with proportional-resonant regulators. Moreover, the design methodology is thoroughly explained when the delay in the calculations is taken into account. In this case, the design procedure allows the dominant poles of the closed-loop system to be chosen. If the closed-loop poles are chosen carefully, this control structure can also be applied to other systems which require higher delays, e.g., power converter applications with a reduced switching frequency. The design methodology can additionally be extended to the discrete domain.

### II-G.1 Design of Two Degrees of Freedom (2DOF)-Resonant Control Scheme

The dynamic behavior can be defined by choosing the location of the desired poles for the closed-loop transfer function. The parameters of the DVR are specified and the delay in the calculations is chosen to be equal to one sampling period with a sampling frequency of 10 kHz, i.e.,  $\tau = 100 \mu s$ . In order to implement the effect of the delay, the Padé approximation of order (n, n) has been used [14], which is defined as:

$$e^{-\tau s} = \frac{\sum_{k=0}^n \binom{n}{k} \frac{(2n-k)!}{(2n)!} (-s\tau)^k}{\sum_{k=0}^n \binom{n}{k} \frac{(2n-k)!}{(2n)!} (s\tau)^k} \quad (21)$$

The fourth-order Padé approximation ( $n = 4$ ) has been used for reasons of computational simplicity.

## III Proposed Approach

Control strategies for a dynamic voltage controller are analyzed with respect to different types of voltage dips. First, symmetrical voltage dips are considered followed by non-symmetrical cases.

### III-A Control Strategy with Symmetrical Voltage Dip

Different control strategies have been evaluated in order to control the DVR. The most commonly used method is to put the DVR voltage in phase with the supply voltage, regardless of the actual phase angle of the load current. An undisturbed load voltage requires this method, but it may lead to a fast drain of the energy storage unit. Energy optimized control has been adapted to save energy and fully utilize the energy storage capacity.

Symmetrical voltage dip are ideally characterized by the dip duration, magnitude reduction and a phase jump. A control strategy for voltage dips with phase jump should be included in order to be able to compensate for this particular type of symmetrical voltage dip. The DVR can be controlled by a number ways to improve certain parameters. It is first assumed, that the DVR is only active during the voltage dip.

1. **Voltage Quality Optimized Control:** The voltages are always compensated to the pre-dip level, disregarding that this may be a operating point with high voltage injection and energy depletion.
2. **Voltage Amplitude Optimized Control:** The injected voltages are controlled in a way, that minimizes the necessary injected voltages.
3. **Energy Optimized Control:** To fully utilize the energy storage, information about the load can be used to minimize the depletion of the energy storage.

The currents and power in steady state absorbed by the load are unchanged:

$$|I_{load}| = \text{constant}, |P_{load}| = \text{constant}, |Q_{load}| = \text{constant} \quad (22)$$

The phase of the load voltages can be changed by the DVR, but with time the phase of the load currents will change until the same active and reactive power are absorbed by the load. The currents are equal for the supply, the DVR and the load and the amplitude of the current depends on the connected load. In a steady-state condition the load will absorb the same amount of power before and during the dip, if the voltage dip is fully compensated. The differences between the three methods are how much power, PDV R and voltage, UDV R the DVR has to inject into the system.

Additionally, the load condition can be expressed by the absorbed apparent power,  $S_{load}$  and the load current,  $I_{load}$ :

$$S_{load} = P_{load} + jQ_{load} \quad (23)$$

The control strategy depends on the type of load connected and the load response to a change in the phase of the impressed voltage. Some loads are very sensitive to a voltage phase shift and a phase shift should be avoided in the control. Other types of loads are more tolerant to phase shifts and the main criteria is to ensure the rated voltage on all three phases.

### III-B Generation of Voltage Dips

The generation of a voltage dip in a strong 10 kV radial is generally ideal and requires a triggering of a short circuit in the grid followed by a clearing of the fault. The maximum voltage dip is generated by connecting the sensitive load at the weakest point at the test site and generate the fault close to the connected DVR. The expected voltage dip is estimated by:

$$U + \text{dip} = U_{supply} \frac{Z_{fault}}{Z_{fault} + Z_{supply}} \quad (24)$$

$$= U_{supply} \frac{Z_{trans}}{Z_{trans} + Z_{supply}} \quad (25)$$

The impedance after the high-voltage transformer to an infinite busbar is estimated to:

$$Z_{inf} = (0 + j0.41) \Omega \quad (26)$$

The supply impedance  $Z_{supply}$  can be altered by connecting or disconnecting existing high-voltage cables or overhead wires in the distribution grid.

## IV Result Analysis

The chapter includes modeling of the dynamic voltage restorer (DVR) system components to be able to simulate the performance of the low-voltage dynamic voltage restorer (LV-DVR) and high-voltage dynamic voltage restorer (HV-DVR). The models have been simulated to present from both the LV-DVR and HV-DVR. Simulations are compared with measurements from the LV-DVR and HV-DVR to verify the models of the DVRs.

## IV-A Simulation and Verification of the System Models

In this section the implemented system model is verified with measurements to ensure, that the DVR is acceptable modelled and that the model implemented can be used to an extensive study of the DVR behavior. First some simulations and measurements are presented for the LV-DVR, and there after for the HV-DVR with the main focus is put on the HV-DVR.

## IV-B Simulation of the LV-DV

The voltage dips are generated by changing the supply voltages. The DVR is simulated with an infinite energy storage and a 0.7 pu symmetrical voltage dip with a 15 negative phase jump. The DVR is loaded with a 5 kW resistive load and the voltage dip takes place at  $t = 50$  ms and is cleared at  $t = 150$  ms. Figure 6 illustrates the simulated response of non-symmetrical voltage dip detection of the LV-DVR. Figure 6 show the initial response of the voltage dip with a

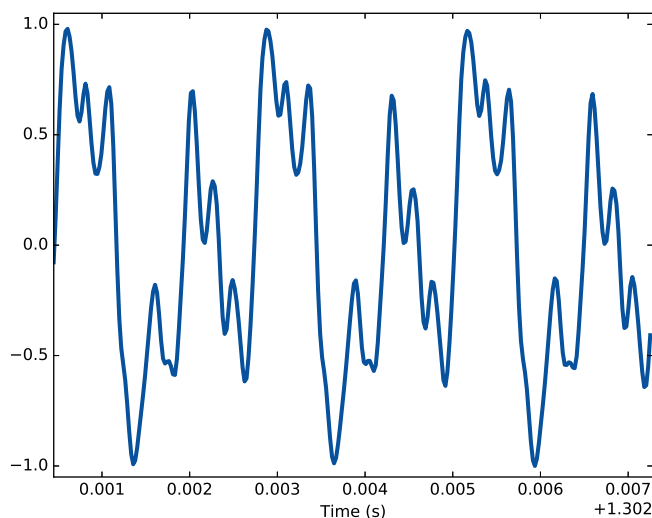


Figure 6: Detection of a Non-Symmetrical Voltage Dip

very ideal step change of the supply voltages. After the dip has been detected by the DVR, it switches from standby operation to active voltage injection and the line-filter oscillations can be seen Figure 6. The control is implemented in the dq-rotating reference frame and the phase jump can be seen by the change in the  $q$ -component of the supply voltage. Both the change in  $d$ -component and  $q$ -component are compensated and the dq-components in the load voltages are restored to  $u_{load}$ ,  $d = 325$  V and  $u_{load}$ ,  $q = 0$  V, respectively.

## IV-C Verification of the LV-DVR Model

A verification of the model is limited to certain operating points within normal operating conditions. The DVR has been simulated under the same conditions, and the two cases have been compared. A zoomed view of the measured response is illustrated in Figure 8 and 8. Both reveal a low-damped oscillation from measurement of the approximate period of the oscillation, and the frequency can be calculated to 1250 Hz. The resonance frequency from the leakage inductance of the transformer and the capacitor in the line-filter can be calculated to 1290 Hz, which explains the origin of the oscillation. The oscillations are weakly damped, because the load is a light resistive load, with a larger load the damping is improved. The oscillations depend also on the phase of the voltage.

## V Conclusion and Future Work

In this paper, novel efficient control management of dynamic voltage restorer using feedback controller have been reported as a major power quality problem and a series connected converter, like the DVR, is considered to be an effective and cost-effective solution to mitigate voltage dips. To gain a better understanding of voltage dip compensation with a dynamic voltage restorer in the distribution grid a number of aspects regarding the dynamic voltage restorer have been analyzed

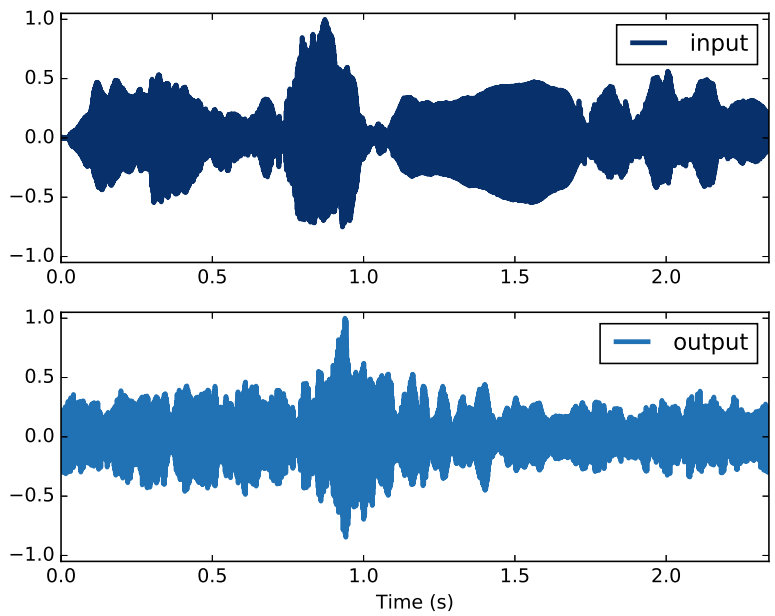


Figure 7: Verification of a Non-Symmetrical Voltage Dip

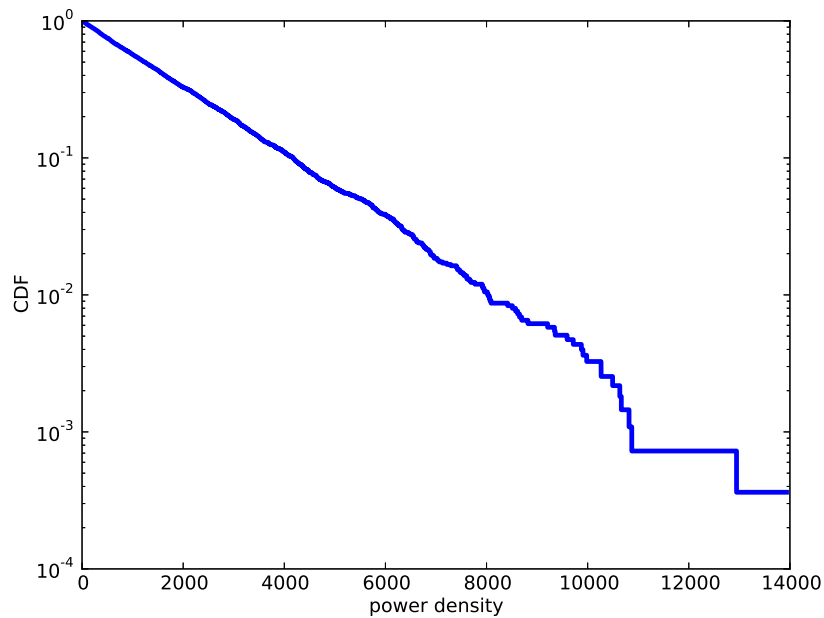


Figure 8: Response of a Non-Symmetrical Voltage Dip

and tested in this paper. In future, verification of the HV-DVR performance at a location with different types of voltage dips can be originated from faults at the transmission level and distribution level. Further investigation of DVR topologies including the direct connected DVR.

## References

- [1] K. Rajkumar, P. Parthiban, and N. Lokesh, "Real-time implementation of transformerless dynamic voltage restorer based on t-type multilevel inverter with reduced switch count," *International Transactions on Electrical Energy Systems*, vol. 30, no. 4, p. e12301, 2020. doi: <https://doi.org/10.1002/2050-7038.12301>
- [2] L. Jian, W. Cao, Y. Jintao, Z. Hao, and L. Xingrui, "Virtual impedance control for a regional dynamic voltage restorer," *International Journal of Electronics*, vol. 105, no. 11, pp. 1881–1899, 2018. doi: <https://doi.org/10.1080/00207217.2018.1494321>
- [3] Y. W. Li, P. C. Loh, F. Blaabjerg, and D. M. Vilathgamuwa, "Investigation and improvement of transient response of dvr at medium voltage level," *IEEE Transactions on Industry Applications*, vol. 43, no. 5, pp. 1309–1319, 2007. doi: <https://doi.org/10.1109/TIA.2007.904430>
- [4] V. E. Puranik, Sabha Raj Arya, and A. Jain, "Comparative study of compensation techniques of dvr with composite observer," in *2016 Biennial International Conference on Power and Energy Systems: Towards Sustainable Energy (PESTSE)*, 2016, pp. 1–7. doi: <https://doi.org/10.1109/PESTSE.2016.7516512>
- [5] R. Pal and S. Gupta, "Topologies and control strategies implicated in dynamic voltage restorer (dvr) for power quality improvement," *Iranian Journal of Science and Technology, Transactions of Electrical Engineering*, vol. 44, no. 2, pp. 581–603, Jun 2020. doi: <https://doi.org/10.1007/s40998-019-00287-3>
- [6] J. G. Nielsen, F. Blaabjerg, and N. Mohan, "Control strategies for dynamic voltage restorer compensating voltage sags with phase jump," in *APEC 2001. Sixteenth Annual IEEE Applied Power Electronics Conference and Exposition*, vol. 2, 2001, pp. 1267–1273. doi: <https://doi.org/10.1109/APEC.2001.912528>
- [7] S. H. Hosseini and M. R. Banaei, "A new minimal energy control of the dc link energy in four-wire dynamic voltage restorer," in *30th Annual Conference of IEEE Industrial Electronics Society, 2004. IECON 2004*, vol. 3, 2004, pp. 3048–3053. doi: <https://doi.org/10.1109/IECON.2004.1432298>
- [8] H. Abdollahzadeh, M. Jazaeri, and A. Tavighi, "A new fast-converged estimation approach for dynamic voltage restorer (dvr) to compensate voltage sags in waveform distortion conditions," *International Journal of Electrical Power & Energy Systems*, vol. 54, pp. 598–609, 2014. doi: <https://doi.org/10.1016/j.ijepes.2013.08.012>
- [9] E. Babaei and M. Farhadi Kangarlu, "A new topology for dynamic voltage restorers without dc link," in *2009 IEEE Symposium on Industrial Electronics Applications*, vol. 2, 2009, pp. 1016–1021. doi: <https://doi.org/10.1109/ISIEA.2009.5356312>
- [10] C. Tu, Q. Guo, F. Jiang, C. Chen, X. Li, F. Xiao, and J. Gao, "Dynamic voltage restorer with an improved strategy to voltage sag compensation and energy self-recovery," *CPSS Transactions on Power Electronics and Applications*, vol. 4, no. 3, pp. 219–229, 2019. doi: <https://doi.org/10.24295/CPSSTPEA.2019.00021>
- [11] A. M. Saeed, S. H. Abdel Aleem, A. M. Ibrahim, M. E. Balci, and E. E. El-Zahab, "Power conditioning using dynamic voltage restorers under different voltage sag types," *Journal of Advanced Research*, vol. 7, no. 1, pp. 95–103, 2016. doi: <https://doi.org/10.1016/j.jare.2015.03.001>
- [12] B. Bae, J. Jeong, J. Lee, and B. Han, "Novel sag detection method for line-interactive dynamic voltage restorer," *IEEE Transactions on Power Delivery*, vol. 25, no. 2, pp. 1210–1211, 2010. doi: <https://doi.org/10.1109/TPWRD.2009.2037520>
- [13] A. P. Torres, P. Roncero-Sánchez, and V. F. Batlle, "A two degrees of freedom resonant control scheme for voltage-sag compensation in dynamic voltage restorers," *IEEE Transactions on Power Electronics*, vol. 33, no. 6, pp. 4852–4867, 2018. doi: <https://doi.org/10.1109/TPEL.2017.2727488>
- [14] J. R. Partington, "Some frequency-domain approaches to the model reduction of delay systems," *Annual Reviews in Control*, vol. 28, no. 1, pp. 65–73, 2004. doi: <https://doi.org/10.1016/j.arcontrol.2004.01.007>